Polym. Korea, Vol. 44, No. 1, pp. 109-115 (2020)
https://doi.org/10.7317/pk.2020.44.1.109

ISSN 0379-153X(Print)
ISSN 2234-8077(Online)

말레산 무수물 그래프트 폴리프로필렌이 재생 탄소섬유 보강 폴리프로필렌에 미치는 영향

안승재 · 연 우 · 전한용*,†

인하대학교 대학원 화학화공융합과, *인하대학교 화학공학과

(2019년 10월 21일 접수, 2019년 11월 6일 수정, 2019년 11월 10일 채택)

Effect of Maleic Anhydride-grafted Polypropylene on Recycled Carbon Fiber Reinforced Polypropylene

SeungJae Ahn, Yu Yan, and Han-Yong Jeon*,†

Department of Chemistry and Chemical Engineering, Inha University, 100 Inha-ro, Michuhol-gu, Incheon 22212, Korea
**Department of Chemical Engineering, Inha University, 100 Inha-ro, Michuhol-gu, Incheon 22212, Korea*

(Received October 21, 2019; Revised November 6, 2019; Accepted November 10, 2019)

초록: 플라스틱 기반 폐기물의 문제가 증가되면서 탄소섬유 복합재료(CFRPs)는 폐순환 재료 수명 주기를 달성할 필요가 있다. 본 연구는 폴리프로필렌(PP)을 사용한 재생 탄소섬유 복합재료(rCFRPs)의 잠재성을 연구하는 것을 목표로 한다. PP는 관능기가 없기 때문에 기계적 물성 향상을 위해 말레산 무수물이 그래프트된 폴리프로필렌(MAPP)을 커플링제로 사용하였다. rCFRP는 재생 탄소섬유(rCF) 습식부직포와 매트릭스 필름을 포개어 압축성형으로 제조하였다. 충분한 산소 관능기가 rCF 표면에 존재함을 확인했으며 그 관능기들은 말레산 무수물(MA)과 rCF 표면의 공유결합에 의한 기계적 물성 향상에 기여하였다. rCFRP의 인장특성은 2 wt%의 MAPP 첨가만으로도 극적인 향상을 보였지만 5 wt%까지 MAPP의 함량에 대한 효과는 미미하였다.

Abstract: As the problem of plastic based material waste is increasing, carbon fiber reinforced plastics (CFRPs) need to achieve closed life cycle. This study aims to investigate the potential for recycled carbon fiber reinforced plastics (rCFRPs) with polypropylene (PP). To improve mechanical properties of rCFRP, maleic anhydride grafted polypropylene (MAPP) was used as a coupling agent due to absence of functional group in PP. The rCFRPs were prepared by compression molding after stacking of recycled carbon fiber (rCF) wet-laid nonwovens and matrix films. The sufficient oxygen functional groups observed on rCF surface and they contributed to improve mechanical properties by covalent bond between maleic anhydride (MA) group and rCF surface. The tensile properties of the rCFRP with 2 wt% MAPP were dramatically increased compared to that without MAPP. However, the effect of MAPP content until 5 wt% on the tensile properties was slight.

Keywords: recycled carbon fiber, wet-laid nonwoven, polymer-matrix composite, coupling agent.

Introduction

Carbon fiber reinforced plastics (CFRPs) can be considered as a strongest potential material to replace not only conventional single polymers but also metallic materials, because carbon fiber (CF) has excellent mechanical, thermal and electrical properties. Although the cost of CF still is high to use many applications,[1] the high value-added industries such as aerospace and automotive are promising markets for CFRPs. CFRPs have a fuel-efficient benefit in vehicles because they are lighter than metallic materials. Moreover the use of CFRPs will be facilitated by the regulations for CO_2 emission reduction that will be strengthened in the future.[2]

However, the use of CFRP is not always expected to have a positive impact on the environment. Recently, plastic waste becomes a new global problem and concerns about CFRPs waste are also growing. Hence, the demands of recycling CFRPs are inevitable, but CFRPs are difficult to recycle due to its complex composition.[3-6] Especially, CFRPs that used the thermoset resins as a matrix are more difficult to recycle in contrast to the case of thermoplastic due to their cross-linked molecular structure.

†To whom correspondence should be addressed.
hyjeon@inha.ac.kr, ORCID 0000-0003-2432-6884

Several attempts to recycle CFRPs have led to the development of various recycling processes.[3-6] The rCF can be obtained with little degradation of mechanical properties compared to virgin CF (vCF). But, except in special cases, most rCFs are reclaimed into short fibers and the diversity of CFRPs waste means that rCF should not be aimed at competing with vCF. The goal of recycled CFRPs (rCFRPs) is to complete the closed life-cycle for CFRPs. Because thermoplastics are easy to reuse and recycle, the matrix more suitable for rCFRP is the thermoplastics rather than thermoset for achieving the goal.

Polypropylene (PP) is a popular commodity thermoplastic for various industrial applications. As a matrix for rCFRP, PP has the advantages that are low cost, easy processing and low weight etc. However, there is concern that PP does not contain a functional group to use as a matrix for rCFRP in which the interfacial adhesion between the recycled CF (rCF) and matrix is an important factor. For improvement interfacial adhesion between fiber and matrix, there are two methods investigated by several studies. First method is a treatment on fiber surface to add functional group.[7,8] The second method is to add a material which contains functional groups to the matrix.[9,10] Physical or chemical surface treatments have been reported to be sufficiently efficient, but there is an issue about the degradation of mechanical properties of rCF.[7,8] Therefore, the latter is considered more suitable for use with rCFRP. Maleic anhydride grafted polypropylene (MAPP) is a coupling agent with maleic anhydride (MA) groups including oxygen functional groups. For various reinforcements such as flax and glass fiber, using MAPP as a coupling agent were proved to improve the mechanical properties of the fiber reinforced PP because the interfacial adhesion increased.[11-16]

In this study, we prepared the rCFRPs with PP and investigated the effects of MAPP content used as coupling agent. The rCF wet-laid nonwovens were incorporated as reinforcements into matrix films by compression molding. In consideration of the impregnation, PP with high melt flow index was selected as the matrix. The compatablized PP pellets were compounded with MAPP coupling agent by single-screw extruder.

Experimental

Materials. The rCF used in this study is purchased from ELG Carbon Fibre Co., Ltd. (U.K.). The fiber length was random distributed and the fiber diameter of rCF was 7.5-8 μm. It was recycled from CFRPs waste through pyrolysis process. Carboxymethyl cellulose sodium salt (CMC-Na) is used as a dispersion agent and it is purchased from Samchun pure chemical Co., Ltd. (Korea). PP (SJ-170) was supplied by Lotte Chemical Co., Ltd. (Korea). The melt flow index of PP at 230 °C is 25 g/10 min and tensile yield strength is 34 MPa according to manufacturer. MAPP (G3003) purchased from Eastman Co., Ltd. (U.K.). The PP was compounded with 2, 3 and 5 wt% of MAPP by single screw extruder.

Preparation of the rCF Wet-laid Nonwovens. For removing very short fibers and dust, the rCFs were washed three times using distilled water in sieve and dried for 24 h at 80 °C. The 4.4 g of rCF was dispersed in the CMC-Na solution that was prepared by sufficiently dissolving the designed weight of CMC-Na in 2 L of distilled water. After dispersion for 10 min at 2700 rpm, the rCF slurry was poured into a square sheet former (25×25 cm^2) filled with 18 L of water. After dispersing for 5 sec with air bubbles, the water was drained to lay the rCF nonwovens. The rCF nonwovens were dried in an oven at 80 °C for 12 h. This process was similar to papermaking (Figure 1) and used the standard disintegrator and square handsheet former according to TAPPI-205.

Manufacturing the rCFRPs. For compression molding, the PP and PP/MAPP pellets were processed into a film. Two layers of the rCF nonwovens and matrix films were cut into squares 18×18 cm^2 respectively and then they were stacked in the closed mold for compression molding as shown Figure 1. The contact pressure was 1 MPa and heat up to 200 °C during 50 min. After pre-heating, the pressure was increased at 10 MPa. After 10 min, the temperature was decreased to room temperature by water cooling system. In the rCFRPs, the fiber volume fraction was about 20%.

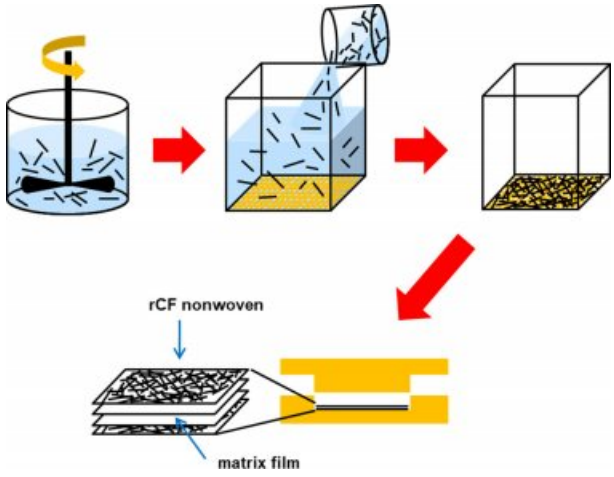

Figure 1. Schematic figure of rCFRP manufacturing process.

Characterization. The morphologies of samples were examined by using scanning electron microscope (SEM, S-3400, Hitachi Co., Ltd., Japan). Before SEM analysis, all the samples were coated with a thin layer of platinum by sputtering for 2 min. SEM with a tungsten filament operated in high vacuum mode at 15 kV. Thermal behaviors of the rCFRPs were observed by using differential scanning calorimetry (DSC, Q20, TA instrument Co., Ltd., USA). Specimens were put into aluminum pans. Under nitrogen atmosphere, the melting temperature (T_m), crystalline temperature (T_c) were measured in the temperature 40 to 200 °C at 10 °C/min of the heat and cooling rate. All the samples were held at 200 °C for 5 min to eliminate thermal history. X-ray photoelectron spectroscopy (XPS, K-alpha, Thermo Fisher Scientific. Inc., USA) was used to investigate the surface chemistry of rCFs. Avantage and XPSPEAK 4.1 software were used to process the spectra. Shirley type background and Gaussian/Lorentzian product functions are applied for C1s high resolution spectra curve fitting. The tensile properties of the rCFRPs were evaluated according to ASTM D 638 'Standard Test Method for Tensile Properties of Plastics' by tensile test using universal test machine (UTM, Instron 3343, Illinois Tool Works Inc., USA). The specimens were cut in the same direction and the cut surface of them was gently sanded with sandpaper. At least 20 specimens of rCFRPs were tested due to large scattered tensile properties and all specimens were tested at crosshead speed of 2 mm/min. Since the specimens were thick (~400 μm), the results of tensile test are only valid for comparison among the samples evaluated.

Results and Discussion

Morphologies of the rCFs. The rCFs consisted of fluffy and bundled types (Figure 2) and the morphologies of the two types of rCFs are shown in Figure 3. It was observed that the surfaces of the receiced rCFs was not clean with contaminants, which were more significantly observed in the rCF bundles compared to rCF fluff. The contaminants are the residual resin and char that were not decomposed during recycling process. Assuming the same recycling process, the mixture state of two types is deduced that the different amount of contaminants in rCFs results from the diversity of raw materials in the CFRPs waste. Giorgini *et al.*[17] have investigated about pyrolysis recycling from CFRP prepreg waste. They have reported that the LDPE films to protect the prepreg induced the more pyrolytic carbon residue. The effect of contaminant on the properties of

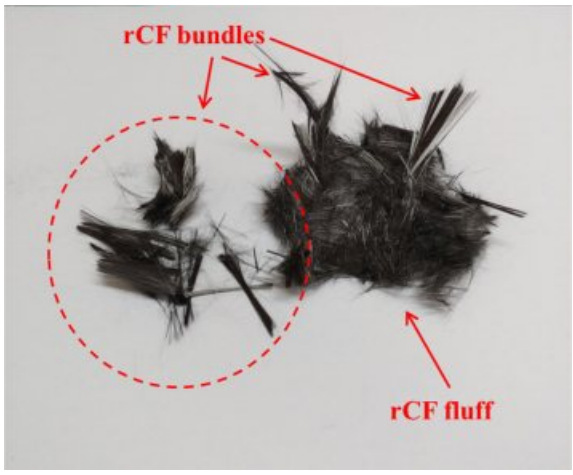

Figure 2. Photograph of as received rCF.

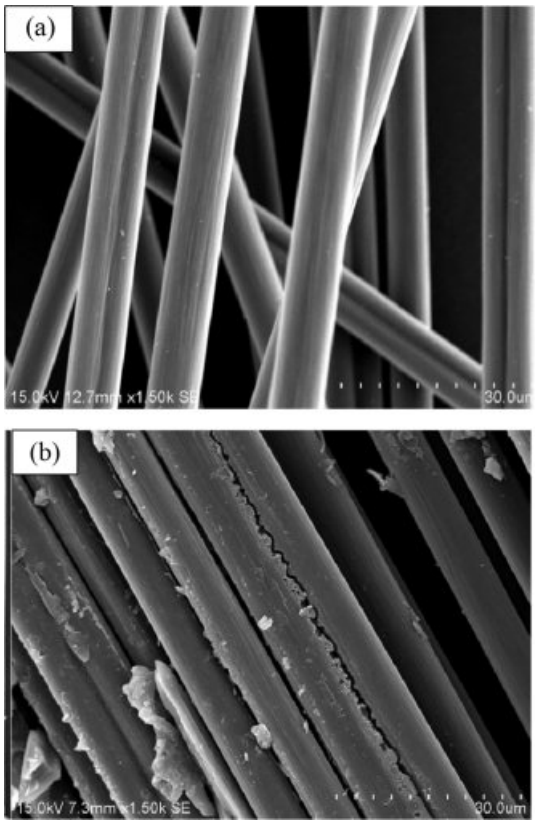

Figure 3. SEM images of (a) rCF fluff; (b) rCF bundle.

rCFRPs should be carefully discussed. Most studies have reported that the contaminant affect the adhesion with new matrix when the rCFRPs would re-manufacture. However, Jiang *et al.*[18] have reported that the mechanical properties of rCF/PP are high compared to that of vCF/PP. They have suggested that the contaminants increase the friction between the

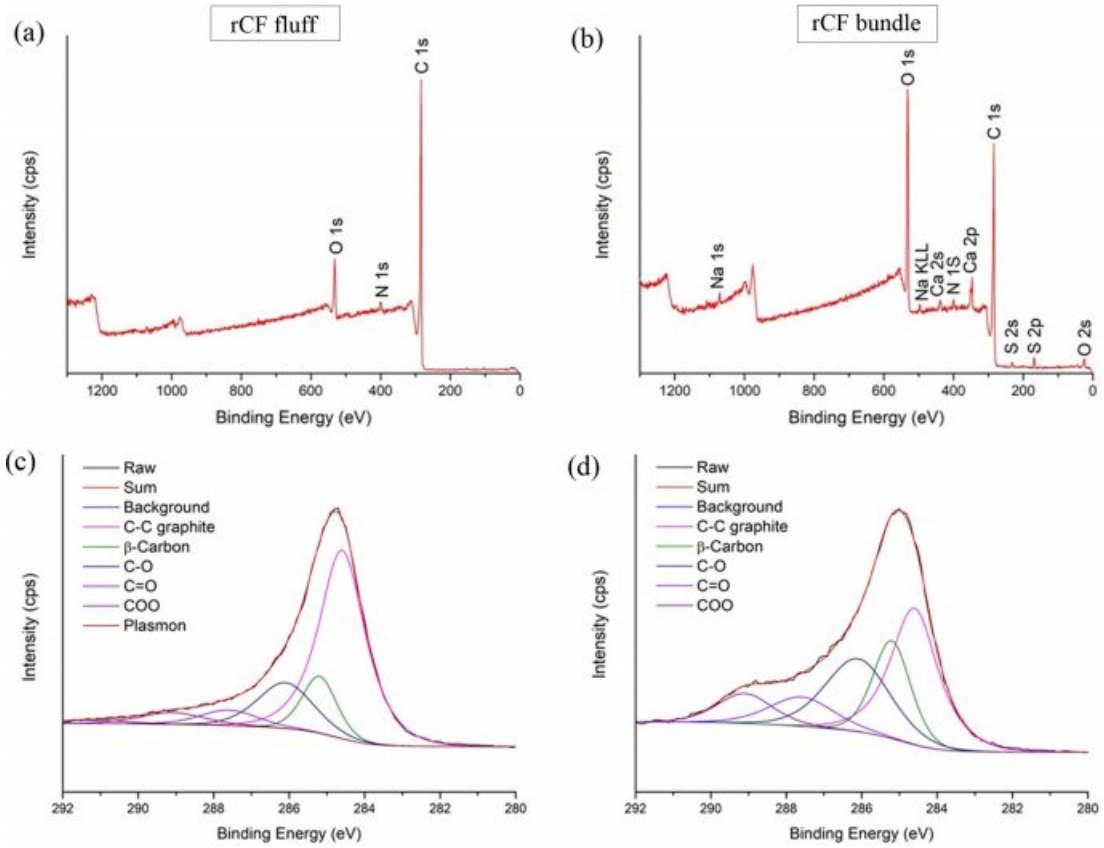

Figure 4. XPS survey spectra (a, b); C1s high resoultion spectra (c, d) of (a, c) rCF fluff and (b, d) rCF bundle.

fiber and matrix, thus improving their tensile strength.

Surface Chemistry of rCFs. For CFRPs, the functional groups on fiber surface are believed to be important in order to improve interfacial adhesion. The effect of MAPP could be expected when there are sufficient functional groups on the rCF surface. Figure 4 shows the XPS survey and the C1s high-resolution spectra of the both rCF types. The oxygen/carbon atomic ratio (O/C) and the curve fitting results are listed in Table 1 and 2. There are the four peaks observed in the XPS survey spectra: the two main peaks carbon (C1s, ~284.4 eV) and oxygen (O1s, ~531.8 eV) and two minor peaks nitrogen (N1s, ~400 eV) and silicon (Si2p, ~102 eV). Furthermore, the non-negligible peaks were observed in the survey spectrum of the bundled rCFs: S2p (~169 eV), S2s (~232 eV), Ca2p (~347 eV), Ca2s (~439 eV) and Na1s (~1071 eV).

Table 1. Atomic Concentration of Various Elements in rCFs

	C (%)	O (%)	N (%)	Si (%)	O/C
rCF fluff	88.07	10.15	0.87	0.91	11.52
rCF bundle	70.17	23.27	2.36	-	33.16

The pyrolysis during recycling process generally takes place in two steps. In the first, the CFRPs waste is pyrolyzed in inert atmosphere.[19,20] The organic matrix is decomposed during this step. In the second, the oxidation step proceeds to remove the remaining matrix residue and pyrolytic carbon after pyrolysis. It has been suggested that the surface oxygen functionalities on rCFs could be removed during the pyrolysis step and then they could be formed during the oxidation step.[20] From the morphology images (Figure 3), it is appropriate to interpret that the

Table 2. Relative Percentages of Functional Groups on the Surface of rCFs

	C-C (graphite)	β-Carbon	C-O	C=O	COO	Plasmon
rCF fluff	59.51	12.47	16.20	5.56	4.74	1.52
rCF bundle	36.77	19.60	24.99	9.95	8.70	-

oxygen functional groups of the fluffy rCF are on fiber surface while those of the bundled rCF are present in the contaminant rather than on the fiber surface. For curve fitting of C1s high-resolution spectra, the first C-C graphitic peak was corrected to 284.6 eV. And then the peaks of β-carbon (carbons adjacent to carbon atoms bonded to oxygen), C-O, C=O, COO and plasmon were assigned to the positions shifted by 0.6, 1.5, 3, 4.5 and 6.7 eV from C-C graphitic peak, respectively.[20-23] In the C1s curve fitting results, the oxygen functionality of the rCFs bundles was higher than that of the rCFs fluff. This results in the increase of β-carbon. Both rCF types have sufficient the O/C values to expect a covalent bond between rCF and MAPP.

Thermal Behaviors of the rCFRPs. The thermograms of the rCFRPs are showed in Figure 5. The slight decrease of the T_m with increasing MAPP content is attributed to the MA group because MA group makes defective crystals.[24,25] It is worth noting that the shoulder melting peak was observed in the 1st heating thermograms of rCFRP with 5 wt% MAPP. Although the all rCFRPs had same thermal history due to manufacturing by same processing, the shoulder peak of the rCFRP with 5 wt% MAPP reveals that the crystallization of their matrix during cooling differs from others. The lower melting peak corresponds to more defective crystal induced by MA groups than the higher melting peak. Also the higher peak could be considered to indicate the melting behavior of the perfect PP crystals which were not influenced by MA groups. Despite the increased MAPP content, the presence of the perfect crystals implies that MA groups are not evenly distributed in the PP. The MA groups would be concentrated in a certain area. The oxygen functional groups on rCF surface would make the MA groups concentrate on the rCF surface. Similar suggestion has been reported in a study by Luo *et al*.[11] As the MAPP content increases, the number of MAPP chains moving to the rCFs surface would increase. These movements could lead to the movements of the longer MAPP chains entangled with short PP chains. And then the MAPP and short PP chains would be concentrated on the rCF surface.

Tensile Properties of the rCFRPs. Figure 6 shows the tensile test results of rCFRPs with different MAPP content. As expected, the results showed that the tensile properties were improved by using PP with MAPP added. For the rCFRP with 2 wt% MAPP, the tensile strength was significantly increased by 113%, the tensile modulus by 26% and the elongation by 56% compared to the rCFRP without MAPP. This significant improvement indicates that MAPP is contributed to the interfacial adhesion between the rCFs and PP. Although the tensile

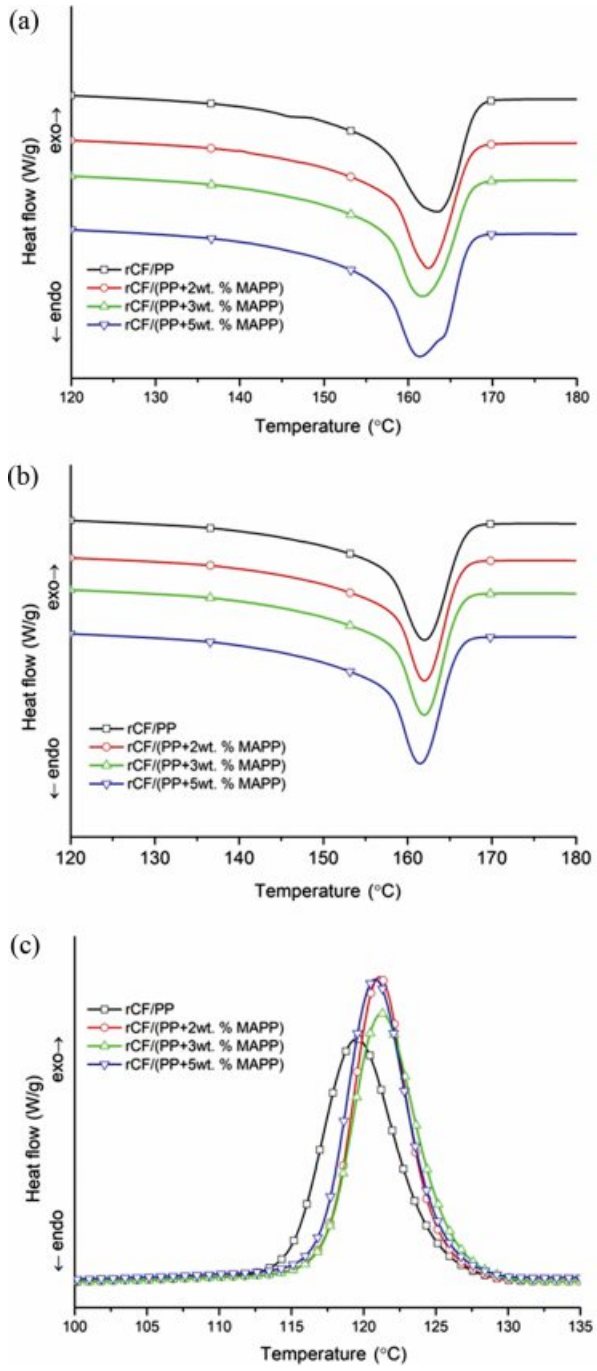

Figure 5. DSC thermograms of rCFRPs: (a) 1st heaing; (b) 2nd heating; (c) 1st cooling.

strength was a maximum value in the rCFRP with 5 wt% MAPP, it is considered that the effect of MAPP content on tensile properties is slight. As MAPP content increased from 2 to 5 wt%, the tensile strength and elongation was increased slightly while the tensile modulus was decreased slightly. This suggests that there is a limit to the improvement of the tensile

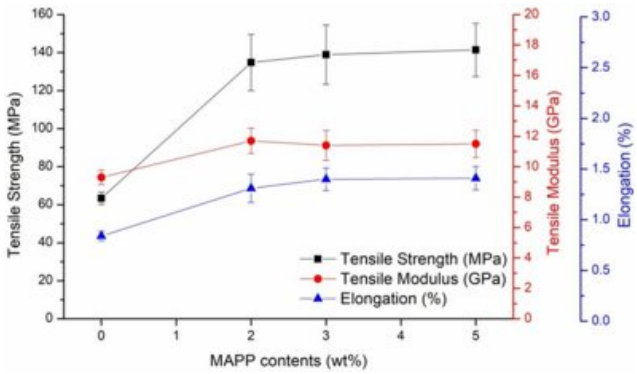

Figure 6. Tensile properites of rCFRPs.

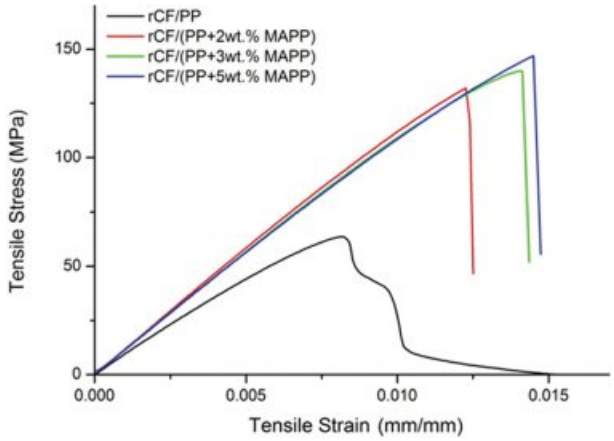

Figure 7. Typical stress-strain curves of the rCFRPs.

properties by the addition of MAPP as reported in many studies.[10-16] The slight effect of MAPP content on the tensile properties is believed to be mainly attributable to excessive density of MAPP and short PP molecular chains on the rCFs surface.

Typical stress-strain curves of the rCFRPs are shown in Figure 7. The tensile behavior of the rCFRP without MAPP was different from the rCFRP with MAPP. The obvious difference in tensile behavior with MAPP addition is after the break point. The tensile stresses of the rCFRP with MAPP were rapidly dropped after break point while tensile stress of the rCFRP without MAPP gradually decreased. The gradual decrease implies that the friction force during the fiber pull-out occurred after the full debonding between the rCF and matrix.

Fractography. Figure 8 shows the fracture surfaces were taken perpendicularly to investigate in detail the MAPP effect contributing to the interfacial adhesion. The length of pulled-out rCFs in rCFRP without MAPP is significant long compared to that with MAPP. The surfaces of pulled-out rCFs in the rCFRP without MAPP are clean, while those with MAPP

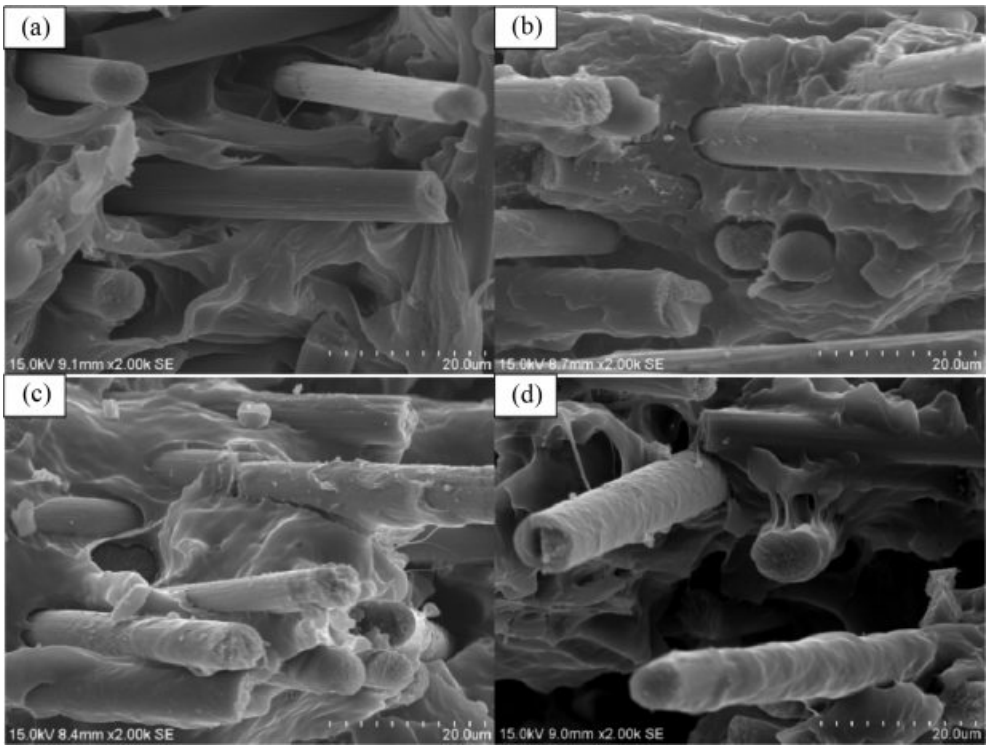

Figure 8. Fracure surfaces of rCFRP taken perpendiculary at high magnification (×2000): (a) rCF/PP; (b) rCF/(PP+2 wt%MAPP); (c) rCF/(PP+3 wt%MAPP); (d) rCF/(PP+5 wt%MAPP).

are covered with the matrix. As the MAPP content increased, the coverage matrix was thicker and frequently observed. The coverage matrix on the rCFs implies the improvement of the interfacial adhesion because the crack induced by the tensile test propagated into matrix instead of the interface between the rCFs and matrix. In particular, it is interesting that the long fibrils are frequently observed on fracture surface in the rCFRP with 5 wt% MAPP. From Figure 8(d), it is deduced that fibrillation is formed from craze-like features between the coverage matrix on the rCFs and the bulk matrix or between the coverage matrices of each adjacent rCFs. The craze-like features would be initiated when the external stretch causes a micro-void to open up at a stress concentration by a heterogeneity in the molecular network.[26] It indicates that the micro-voids are favorable to be created where molecular entanglement density is relatively low, and that their position results in the thickness of the coverage matrix on the rCFs surface. Furthermore, the craze-like features and fibrils indicate that enough molecular entanglement exists on the vicinity of rCFs in the rCFRP with 5 wt% MAPP. This finding supports the molecular entanglement was induced by the excessive MAPP molecular density, which was discussed for the shoulder melting peak in 1st heating thermogram of rCFRP.

Conclusions

The rCFs and the rCF nonwovens incorporated into PP by compression molding have been investigated. Furthermore, in order to improve the tensile properties, the effect of MAPP on the composite has been also investigated. The rCF is consisting of two types: fluffy and bundled rCF. Both types have sufficient oxygen functional groups on fiber surfaces and MA group in MAPP could react for covalent bond to fiber surface. The 2 wt% addition of MAPP resulted in dramatic improvement of tensile properties, but the effect of the MAPP content was small. The slight effect has been considered to be associated with excessive molecular chain density on the rCF surface. In the rCFRP with 5 wt% addition of MAPP, the excessive molecular chain density is implied by the shoulder peak in DSC analysis and by the craze-like features in fracture morphology. Finally, it is seen that the shoulder peak is due to the excessive chain density through DSC analysis result.

Acknowledgements: This work was supported by 2019 INHA UNIVERSITY Research Grant.

References

1. D. A. Baker and T. G. Rials, *J. Appl. Polym. Sci.*, **130**, 713 (2013).
2. T. Ishikawa, K. Amaoka, Y. Masubuchi, T. Yamamoto, A. Yamanaka, M. Arai, and J. Takahashi, *Compos. Sci. Technol.*, **155**, 221 (2018).
3. S. J. Pickering, *Composites Part A*, **37**, 1206 (2006).
4. S. Pimenta and S. T. Pinho, *Waste Manage.*, **31**, 378 (2011).
5. G. Oliveux, L. O. Dandy, and G. A. Leeke, *Prog. Mater. Sci.*, **72**, 61 (2015).
6. F. Meng, J. McKechnie, T. Turner, K. H. Wong, and S. J. Pickering, *Environ. Sci. Technol.*, **51**, 12727 (2017).
7. A. Greco, A. Maffezzoli, G. Buccoliero, F. Caretto, and G. Cornacchia, *J. Compos. Mater.*, **47**, 369 (2013).
8. H. Lee, I. Ohsawa, and J. Takahashi, *Appl. Surf. Sci.*, **328**, 241 (2015).
9. M. Szpieg, K. Giannadakis, and L. E. Asp, *J. Compos. Mater.*, **46**, 1633 (2012).
10. K. H. Wong, D. S. Mohammed, S. J. Pickering, and R. Brooks, *Compos. Sci. Technol.*, **72**, 835 (2012).
11. G. Luo, W. Li, W. Liang, G. Liu, Y. Ma, Y. Niu, and G. Li, *Compos. Part-B Eng.*, **111**, 190 (2017).
12. A. Arbelaiz, B. Fernandez, J. A. Ramos, A. Retegi, R. Llano-Ponte, and I. Mondragon, *Compos. Sci. Technol.*, **65**, 1582 (2005).
13. A. R. Sanadi, D. F. Caulfield, R. E. Jacobson, and R. M. Rowell, *Ind. Eng. Chem. Res.*, **34**, 1889 (1995).
14. W. Qiu, T. Endo, and T. Hirotsu, *Eur. Polym. J.*, **42**, 1059 (2006).
15. A. K. Rana, A. Mandal, and S. Bandyopadhyay, *Compos. Sci. Technol.*, **63**, 801 (2003).
16. B. A. Acha, M. M. Reboredo, and N. E. Marcovich, *Polym. Int.*, **55**, 1104 (2006).
17. L. Giorgini, T. Benelli, L. Mazzocchetti, C. Leonardi, G. Zattini, G. Minak, E. Dolcini, M. Cavazzoni, I. Montanari, and C. Tosi, *Polym. Compos.*, **36**, 1084 (2015).
18. L. Jiang, C. A. Ulven, D. Gutschmidt, M. Anderson, S. Balo, M. Lee, and J. Vigness, *J. Appl. Polym. Sci.*, **132**, 42658 (2015).
19. L. O. Meyer, K. Schulte, and E. Grove-Nielsen, *J. Compos. Mater.*, **43**, 1121 (2009).
20. G. Jiang and S. J. Pickering, *J. Mater. Sci.*, **51**, 1949 (2016).
21. E. Desimoni, G. I. Casella, A. Morone, and A. M. Salvi, *Surf. Interface Anal.*, **15**, 627 (1990).
22. W. H. Lee, J. G. Lee, and P. J. Reucroft, *Appl. Surf. Sci.*, **171**, 136 (2001).
23. Y. Wang, H. Viswanathan, A. A. Audi, and P. M. Sherwood, *Chem. Mater.*, **12**, 1100 (2000).
24. K. Cho, F. Li, and J. Choi, *Polymer*, **40**, 1719 (1999).
25. Y. Seo, J. Kim, K. U. Kim, and Y. C. Kim, *Polymer*, **41**, 2639 (2000).
26. R. A. C. Deblieck, D. J. M. van Beek, K. Remerie, and I. M. Ward, *Polymer*, **52**, 2979 (2011).